Passive Prandtl-Meyer Expansion Flow with Homogeneous Condensation

Seung-Cheol Baek, Soon-Bum Kwon
Department of Mechanical Engineering, Kyungpook National University, 1370, Sankyuk-dong, Daegu 702-701, Korea
Heuy-Dong Kim*
School of Mechanical Engineering, Andong National University, Songchun-dong, Andong 760-749, Korea

Prandtl-Meyer expansion flow with homogeneous condensation is investigated experimentally and by numerical computations. The steady and unsteady periodic behaviors of the diabatic shock wave due to the latent heat released by condensation are considered with a view of technical application to the condensing flow through steam turbine blade passages. A passive control method using a porous wall and cavity underneath is applied to control the diabatic shock wave. Two-dimensional, compressible Navier-Stokes with the nucleation rate equation are numerically solved using a third-order TVD (Total Variation Diminishing) finite difference scheme. The computational results reproduce the measured static pressure distributions in passive and no passive Prandtl-Meyer expansion flows with condensation. From both the experimental and computational results, it is found that the magnitude of steady diabatic shock wave can be considerably reduced by the present passive control method. For no passive control, it is found that the diabatic shock wave due to the heat released by condensation oscillates periodically with a frequency of 2.40 kHz. This unsteady periodic motion of the diabatic shock wave can be completely suppressed using the present passive control method.

Key Words: Compressible Flow, Condensation, Diabatic Shock Wave, Passive Control Prandtl-Meyer Flow

Nomenclature

C_p : Specific heat at constant pressure [J/(kg·K)]
D : Depth of cavity [mm]
E_t : Total energy per unit volume [J/m^3]
E, F: Numerical flux
f : Frequency [kHz]
g : Condensate mass fraction
h^* : Tube height [mm]
H : Source term
I : Nucleation rate [1/(m^3·s)]
J : Jacobian
k : Boltzmann constant [J/K]
L : Latent heat [J/kg], length of cavity [mm]
m : Mass [kg] or molecular weight [kg/kmol]
Pr : Prandtl number
p : Static pressure [Pa]
p_∞ : Flat film equilibrium vapour pressure [Pa]
Q : Conservation mass term
R, S: Viscous term
Re : Reynolds number
R : Gas constant [J/(kg·K)]
r : Droplet radius [m]
r_c : Critical droplet radius [m]
S : Degree of supersaturation
t : Time [s] or temperature [℃]

* Corresponding Author,
E-mail : kimhd@andong.ac.kr
TEL : +82-54-820-5622; **FAX** : +82-55-823-5495
School of Mechanical Engineering, Andong National University, Songchun-dong, Andong 760-749, Korea.
(Manuscript **Received** June 25, 2003; **Revised** January 8, 2004)

T : Temperature [K]
u, v : Cartesian velocity components [m/s]
x_c : Distance from the exit of the edge of backward-facing step [mm]
x_p : Distance from the nozzle throat to the of the cavity [mm]
x, y : Cartesian coordinates [m]

Greek symbols

γ : Specific heat ratio
Γ : Accommodation coefficient of nucleation
ς : Coefficient of surface tension
μ : Dynamic viscosity [Pa·s]
ξ, η : Generalized coordinates
ξ : Condensation coefficient
ρ : Density [kg/m^3]
σ : Surface tension [N/m]

Sub/superscripts

01 : Stagnation state
∞ : Infinite plane surface
l : Liquid
m : Mixture
r : Droplet radius
v : Vapour

1. Introduction

Supersonic flow with heat addition has long been a subject of the physical sciences and engineering technology, and its typical application is often found in blade passages of steam turbine and over a flight body flying into moist atmospheric air. In usual, rapid expansion of moist air or steam through a supersonic nozzle or a turbine cascade leads to condensation phenomenon (Wegener and Mack, 1958 ; Matsuo et al., 1985 ; Schnerr, 1986). In the region that the supersaturated water vapor condenses, the heat released by condensation is added to the flow field, resulting in a significant influence on the whole flow field. Such a condensation phenomenon is essentially made as a nonequilibrium process due to an extremely rapid expansion of moist air. It has been well known that, as the heat release is over a critical value, a diabatic shock wave occurs in the condensation process (Wegener and Mack, 1958 ; Matsuo et al., 1985 ; Schnerr, 1986).

The diabatic shock wave due to the heat released by condensation process has been often found in a vicinity of the trailing edge of blades in steam turbine, significantly affecting the downstream wake flows. Such a condensation phenomenon is a thermodynamically irreversible process resulting in the production of entropy that consequently translates into a remarkable reduction in turbine efficiency. For instance, the steam enters the low-pressure turbine cascade blades as a dry superheated vapor, but it exhausts as two-phase mixture of saturated vapour and condensation liquid droplets. In such a situation, the flow becomes supersonic and generates shock waves that can interact in a highly complex way with the condensation processes of droplet nucleation and growth. Sometimes the condensation effects are comparable to or even greater than the conventional turbulent viscous losses (White et al., 1996 ; Walters, 1985). This makes turbine design extremely difficult.

Many experimental researches have been performed to investigate the characteristics of the nonequilibium condensation process in supersonic nozzle (Wegener and Mack, 1958; Matsuo et al., 1985 ; Wegener and Pouring, 1964 ; Wegener and Cagliostro, 1973 ; Matsuo et al., 1985). According to these works, it has been well documented that the steady and unsteady diabatic shock waves occur in a narrow region of nonequilibrium condensation downstream of the nozzle throat, being very sensitive to the nozzle supply conditions, and these result in a periodic motion that leads to noise and vibration problems in flow passage.

In addition to the nozzle flows, condensation phenomenon can also occur in unsteady expansion wave in the driver section in a shock tube and in Prandtl-Meyer corner flows. Many experimental studies have been made to explore the condensation phenomenon in the shock tube flows (Kalra, 1975 ; Kawada and Mori, 1973 ; Peters, 1987 ; Peters and Paikert, 1989). Sislian and Glass (1976) have used the numerical method of characteristics to solve the condensation flow in shock tube. Smith (1971), Kurshakov et al. (1971) and Frank (1979, 1985) have experiment-

ally and numerically investigated the Prandtl-Meyer expansion flows with homogeneous condensation. These experiments mainly concentrated on measurements of the condensation onset conditions, whereas the numerical solutions employed the method of characteristics in the absence of the diabatic shock wave, which is produced when the amount of heat released by condensation exceeds a critical value.

Delale and Crighton (1998, 2001) have employed an asymptotic method to solve subcritical and supercritical Prandtl Meyer corner flows with homogeneous condensation, and they have reported the diabatic shock behaviors with various supply relative humidities, with the rest of the supply conditions held fixed. White et al.(1996) have made extensive experimental work to get insight into the condensation phenomenon in Prandtl-Meyer flows, which are able to apply the condensing flow through steam turbine blade passages. They have investigated the flow parameters influencing on the steady and unsteady non-equilibrium condensation. They have further performed a dimensional analysis to describe the onset of condensation, the corresponding adiabatic supercooling and the frequency of the unsteady and periodic condensation process. Furthermore, they have estimated the components of energy loss, occurring in the condensing flow, which are divided into three components of shock wave plus wetness loss, viscous loss and mixing loss. As a consequence, they have argued that the thermodynamic component of the total wetness loss in the nucleating stage of the steam turbine can be of comparable magnitude to the viscous loss. They have further reproduced the experimental results using two-dimensional Euler equations and have predicted the surface pressure distributions on the turbine blades with close agreement with the measured pressures, but they have found no sign of the periodic unsteady flow in the steam turbine blades, as often found in supersonic nozzles with condensation.

Frank (1985) has experimentally investigated the diabatic shock behavior in the Prandtl-Meyer corner expansion flows and was the first to show the unsteady diabatic shock motions. However, he did not discuss about the time-dependent condensation flow properties. None of the numerical and experimental investigations performed to date are sufficient in satisfactorily describing Prandtl-Meyer expansion flows with condensation and further investigations need to be pursued.

Meanwhile, the condensation phenomenon may be applied to control the shock wave boundary interaction phenomena at transonic and supersonic speeds, since the condensation process causes the local static pressure of flow to increase and thereby decelerate the flow speed, leading to a reduction in the magnitude of the shock wave interacting with wall boundary layers. Until now, a number of works have performed to control shock wave boundary layer interaction. Typical example is a passive control method using a porous wall and cavity system (Bahi et al., 1983 ; Raghunathan, 1989). According to these works, it has been documented that the shock wave boundary layer interaction is considerably alleviated as the passive porous and cavity system is applied at the foot of the shock wave.

The present study are to investigate the Prandtl-Meyer expansion flows with homogeneous condensation experimentally and by numerical computations and to explore the porous wall and cavity system for the purpose of control of the diabatic shock wave due to the heat released by condensation. Both experimental and computational methods are adopted to investigate the major features of the steady and unsteady periodic condensation flow. Experimentation is carried out using an indraft supersonic wind tunnel. Flow visualization and pressure measurements are conducted to specify the passive Prandtl-Meyer expansion flow with condensation. Two-dimensional Navier-Stokes equations, which are combined the nucleation rate equation with a droplet growth equation, are solved using a third-order TVD (Total Variation Diminishing) finite difference scheme. The present computational attempt is the first to simulate the steady and unsteady periodic behaviors in passive Prandtl-Meyer expansion flow with homogeneous condensation.

2. Experimental Work

Moist air at atmospheric conditions in the plenum chamber flows through a test section into a vacuum chamber having a volume of 10 m^3. A two-dimensional convergent nozzle is installed into the test section of a duct of 60 mm high and 38 mm wide, and it has a height of $h^*=20$ mm at the exit, as schematically shown in Fig. 1. A cavity is installed on the upper wall downstream of the exit of the convergent nozzle, its length L being varied to give different cavity volumes, but its depth is held constant at $D=5$ mm. A porous plate that has a thickness of 1.0 mm consists of a multiple of two-dimensional slots, and it covers the cavity plenum, and the width between the slots is held constant at $w=1.0$ mm. The resulting porosity of the porous wall (slotted wall) is kept constant at 0.18.

In order to change the location of the cavity relative to the nozzle exit, x_c and x_p are defined as the distances from the nozzle exit to the backward-facing step and from the nozzle exit to the leading edge of the cavity, respectively.

The stagnation pressure p_{01} and temperature T_{01} of moist air in the upstream plenum chamber is kept constant at 101.3 kPa and 298 K, respectively. The relative humidity of moist air is varied using a vapour generator system installed inside the plenum chamber, giving different values of the initial degree of supersaturation S_{01} (i.e., the ratio of vapor pressure to equilibrium saturation pressure). A multiple of static holes are drilled into the side-wall of the test section and the array of the static holes is located at 15 mm away from the bottom wall of the convergent nozzle. Pressure transducers (TOYODA, PMS-5H) flush mounted on the side-wall are employed to measure static pressures of the Prandtl-Meyer expansion flow with condensation.

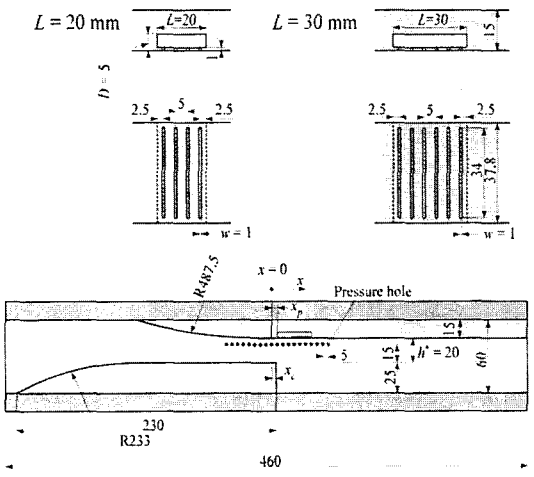

Fig. 1 Details of test section (unit : mm)

An analog-to digital converter, in conjunction with a personal computer, records the amplified output from the transducers to an x-y recorder system. The pressure transducers are calibrated both statically and dynamically, before experiments. Using the calibration information, the error associated with the pressure measurements is estimated to be approximately 1.0%, based on the experimental uncertainty analysis. These estimations are based on the maximum possible fluctuations in the measurements.

Schlieren optical methods are employed for visualization of the condensing flow field through Prandtl-Meyer corner expansion. Mg spark lamp, which has a flash duration of about 2 microseconds, is used to obtain the flow field at any instant.

3. Computational Analysis

Computational predictions for comparison with the experimental measurements are performed using two-dimensional Navier-Stokes equations, which are combined the nucleation rate equation with a droplet growth equation. The present computations used neglect interphase velocity and temperature slip, which is a good approximation for homogeneous condensation droplets like in the present study. It is assumed that the condensation particles have a negligible effect on pressure field. The conservation equations of mass, momentum and energy for the viscous adiabatic compressible flow of the mixture are given being similar to their single phase flow. Mathematical closure of these equations requires a separate equation for the wetness fraction and

this is obtained from the theories of condensation and droplet growth. The resulting governing equation systems are written by

$$\frac{\partial Q}{\partial t}+\frac{\partial E}{\partial x}+\frac{\partial F}{\partial y}=\frac{1}{\mathrm{Re}}\left(\frac{\partial R}{\partial x}+\frac{\partial S}{\partial y}\right)+H \quad (1)$$

where

$$Q=\begin{bmatrix}\rho_m\\ \rho_m u\\ \rho_m v\\ \rho_m E_t\\ \rho_m g\\ \rho_m D_1\\ \rho_m D_2\\ \rho_m D_3\end{bmatrix},\ E=\begin{bmatrix}\rho_m u\\ \rho_m u^2+p\\ \rho_m uv\\ u(E_t+p)\\ \rho_m ug\\ \rho_m uD_1\\ \rho_m uD_2\\ \rho_m uD_3\end{bmatrix},\ F=\begin{bmatrix}\rho_m v\\ \rho_m v\\ \rho_m v^2+p\\ v(E_t+p)\\ \rho_m vg\\ \rho_m vD_1\\ \rho_m vD_2\\ \rho_m vD_3\end{bmatrix}, \quad (2)$$

$$R=\begin{bmatrix}0\\ \tau_{xx}\\ \tau_{xy}\\ \alpha\\ 0\\ 0\\ 0\\ 0\end{bmatrix},\ S=\begin{bmatrix}0\\ \tau_{yx}\\ \tau_{yy}\\ \beta\\ 0\\ 0\\ 0\\ 0\end{bmatrix},\ H=\begin{bmatrix}0\\ 0\\ 0\\ 0\\ \rho_m\dot{g}\\ \rho_m\dot{D}_1\\ \rho_m\dot{D}_2\\ \rho_m\dot{D}_3\end{bmatrix}$$

In these equations,

$$E_t=\rho_m C_{p0}T-p+\frac{1}{2}\rho_m(u^2+v^2)-\rho_m gL \quad (3)$$

$$\alpha=u\tau_{xx}+v\tau_{yx}+\frac{\mu}{(\gamma-1)\,\mathrm{Pr}}\frac{\partial T}{\partial x} \quad (4)$$

$$\beta=u\tau_{xy}+v\tau_{yy}+\frac{\mu}{(\gamma-1)\,\mathrm{Pr}}\frac{\partial T}{\partial y} \quad (5)$$

$$p=G\left[E_t-\frac{1}{2}\rho_m(u^2+v^2)+\rho_m gL\right] \quad (6)$$

$$G=\left(1-g\frac{M_m}{M_v}\right)\Big/\left(\frac{1}{\gamma-1}+g\frac{M_m}{M_v}\right) \quad (7)$$

$$L=2.353\times10^6-5.72\times10^4(\ln p-10)-4.60\times10^3(\ln p-10)^2\ \ (\mathrm{J/kg}) \quad (8)$$

τ_{xx}, τ_{xy}, τ_{yx} and τ_{yy} above are components of viscous shear stresses. $g=(m_l/(m_a+m_v+m_l))$ is condensate mass fraction. Subscript m refers to the mixture. g, D_1, D_2, and D_3 are given as follows;

$$\dot{g}=\frac{dg}{dt}=\frac{\rho_l}{\rho_m}\frac{4\pi}{3}\left(r_c^3 I+\rho_m D_1\frac{\partial r}{\partial t}\right) \quad (9)$$

$$\dot{D}_1=\frac{dD_1}{dt}=\frac{4\pi r_c^2 I}{\rho_m}+D_2\frac{dr}{dt} \quad (10)$$

$$\dot{D}_2=\frac{dD_2}{dt}=\frac{8\pi r_c^2 I}{\rho_m}+D_3\frac{dr}{dt} \quad (11)$$

$$\dot{D}_3=\frac{dD_3}{dt}=\frac{8\pi I}{\rho_m} \quad (12)$$

The rate of formation of condensation droplet embryos per unit mass of mixture I, the critical radius of the condensation nuclei r_c and the radius growth rate $\dot{r}$ are obtained from the classical theories of homogeneous condensation as

$$I_F=\Gamma\cdot I \quad (13)$$

$$I=\frac{1}{\rho_l}\left(\frac{p_v}{kT}\right)^2\sqrt{\frac{2\sigma M_v}{N_A\pi}}\exp\left\{\frac{-4\pi\sigma r_c^2}{3kT}\right\} \quad (14)$$

$$r_c=\frac{2\sigma}{\rho_l\Re T\ \ln(p_l/p_\infty)} \quad (15)$$

$$\dot{r}=\frac{dr}{dt}=\frac{\xi_c}{\rho_l}\frac{p_\infty}{\sqrt{2\pi\Re T}}\left(\frac{p_v}{p_\infty}-1\right) \quad (16)$$

$$p_\infty=10^{(-A/T+B)}\times101325\ \ (\mathrm{Pa}) \quad (17)$$

In Eq. (13) an accommodation coefficient, Γ is assumed to be unity in the present computations and in Eq. (17), A and B are constants depending on the medium gas temperature which are defined next:

$A=2263$, $B=6.064$ for $T=273\sim395$ K
$A=2672$, $B=7.582$ for $T=175\sim273$ K

In the equations above, M, $\Re$, k, p_∞ are molecular weight, gas constant, Boltzmann constant and flat film equilibrium vapour pressure, respectively. Subscripts v and l refer to vapour and liquid phases, respectively. In Eq. (15), ξ_c is a condensation coefficient. Surface tension σ is given using the surface tension of an infinite flat-film σ_∞ and the coefficient of surface tension ζ,

$$\sigma=\zeta\sigma_\infty \quad (18)$$

$$\sigma_\infty=(128-0.192T)\times10^{-3}\ \ (\mathrm{N/m}) \quad (19)$$

In computations, the values chosen for ξ_c and ζ are assumed to be 0.1 and 1.22, respectively (Adam and Schnerr, 1997). Baldwin-Lomax

model (Baldwin and Lomax, 1978) is employed to solve turbulence stresses. A third-order TVD (total variation diminishing) finite difference scheme with MUSCL (Yee 1989) is used to discretize the spatial derivatives of the governing equations and a second-order central difference scheme is applied to the viscous terms. A second-order fractional time step is employed for the time integration.

The governing equation systems above are mapped from the physical plane (x, y) into a computational plane (ξ, η) on which is made of the rectangular mesh computational grids, as shown in Fig. 2. The fineness of computational grids was examined to assure that the obtained solutions were independent of the grid employed. The grids are clustered in regions with large gradients, such as shock waves, boundary layers, so that those provide more reasonable predictions. The resulting computational grids are 375×142 in the x and y directions, respectively. The computational grids closest to the solid walls are located at 0.00154 mm away from the walls.

In the present computations, the values of the initial degree of supersaturation $s_{01}(=p_{v0}/p_{01})$ of moist air are held fixed at 0.6 and 0.9 in the upstream plenum chamber. Inlet and exit boundaries are constrained to the free-boundary conditions. No-slip velocity is assumed on the solid wall surfaces, which are in adiabatic condition of no heat transfer. Further, condensate mass fraction $g=0$ is given at the wall surfaces.

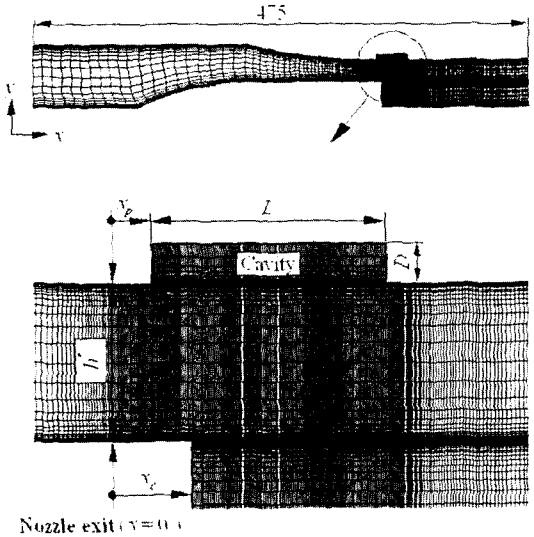

Fig. 2 Computational grid (Unit : mm)

4. Results and Discussion

Figures 3 and 4 show typical schlieren pictures of the passive and no passive Prandtl-Meyer expansion flow field with homogeneous condensation, where $S_{01}=0.6$, the cavity length L is varied by $L=20$ mm and 30 mm, respectively, and the flow direction is left to right. In both figures, x_p is fixed at 5 mm, but x_c is varied. For reference, the schlieren pictures are also presented for the solid upper wall. It is clear that for the solid wall, a diabatic shock wave due to the heat released by condensation occurs inside Prandtl-Meyer expansion fan. For the passive upper wall, the Mach waves generated from the slots of the porous wall interact with the diabatic shock wave and the shear layers that are produced from the edge of the backward-facing step.

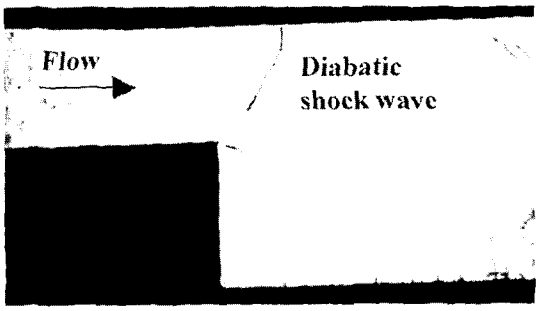

(a) Solid wall

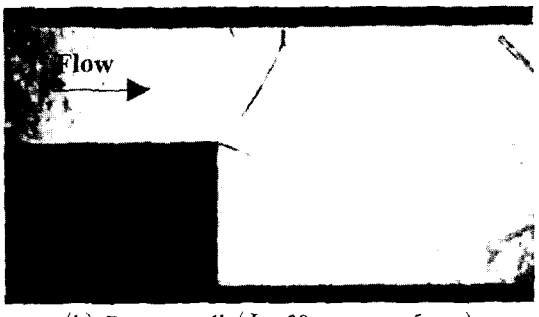

(b) Porous wall ($L=20$ mm, $x_p=5$ mm)

Fig. 3 Schlieren pictures ($S_{01}=0.6$, $x_c=5$ mm)

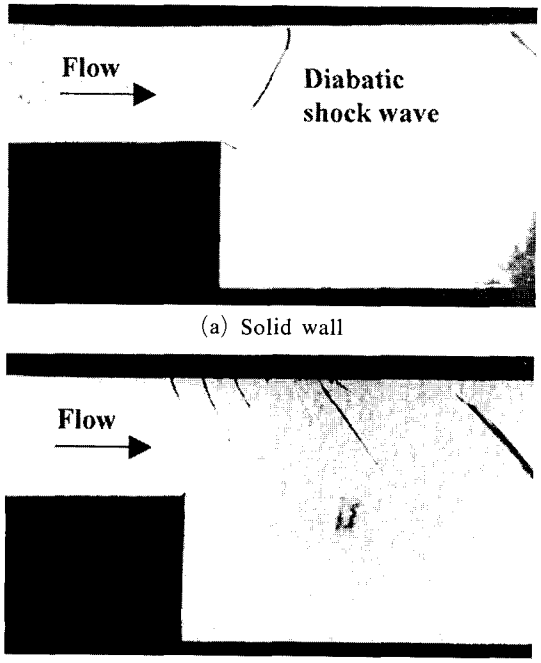

(a) Solid wall

(b) Passive wall (L=30 mm, x_p=5 mm)

Fig. 4 Schlieren pictures (S_{01}=0.6, x_c=10 mm)

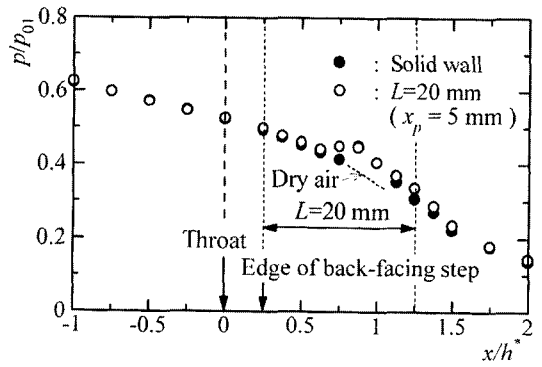

(a) L=20 mm, x_c=5 mm

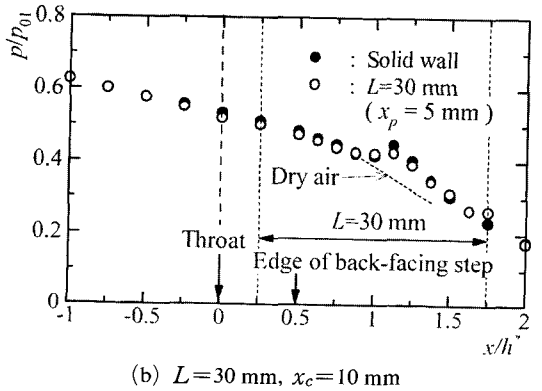

(b) L=30 mm, x_c=10 mm

Fig. 5 Static pressure distribution (S_{01}=0.6)

Figure 5 shows experimental static pressure distributions, where x is the distance from the nozzle exit, L is 20 mm and 30 mm, x_p is 5 mm, and the local static pressure p is presented in a non-dimensional form using the stagnation pressure p_{01} in the upstream plenum. The closed and open circles in the figure indicate the static pressures for the condensing air flow measured through static holes on side wall, and the dotted line is for Prandtl-Meyer expansion flow without condensation. The static pressure distribution for dry air flow within the expansion fan decreases continuously. However for solid wall, the static pressure decreases with x and it abruptly increases when the flow meets the diabatic shock wave due to condensation. Then the static pressure decreases again monotonously. For the passive wall, the static pressure jump due to the heat released by condensation becomes weaker, compared with the solid wall case. The static pressure distributions do not show a sharp discontinuity of the diabatic shock wave, due to a spatial limit in installing the static holes. The sharp pressure rise is much more mitigated for the case of L= 30 mm than L=20 mm. The stronger effectiveness of present passive control method to mitigate the shock strength is confirmed by observing the aforementioned schlieren pictures in Figs. 3 and 4.

In experiment, the cavity location x_c was varied to investigate the pressure jump due to the diabatic shock wave. This was because the flow is very sensitive to the location of the diabatic shock wave relative to the porous wall. As a consequence, the pressure jump was most reduced when the diabatic shock wave was located at the mid (i.e., $L/2$) of the porous wall and its reduction was about 10% of the pressure jump for the solid upper wall.

For both the passive and solid walls, Figs. 6 and 7 show the computed results of Prandtl-Meyer expansion flow with condensation, where S_{01}=0.6. In the density contour maps, the values of $\Delta\rho$ are indicated by a dimensionless quantity relative to the density at the plenum conditions. It is observed that the computed results are in close agreement with the schlieren pictures. For the

solid wall, the diabatic shock wave occurs inside the expansion fan downstream of the nozzle exit, and it seems to be very weak and nearly normal to the upper wall. For the passive wall, the diabatic shock wave is not clearly observed, but a multiple of expansion and compression waves are produced at the slots of the porous wall. It is also found that strong condensate mass fractions are concentrated mainly in the Prandtl-Meyer expansion fan, the upper wall boundary layer and the shear layers. It is interesting to note that considerable condensate mass fraction is also formed inside the recirculation region of the backward-facing step.

For solid wall, the condensate mass fraction in the Prandtl-Meyer expansion fan is formed in a narrow region, forming a condensation zone that seems to be concave with respect to the oncoming flow. The passive wall causes such a condensate mass fraction to distribute spatially over a wide range. It is worthwhile noting that near the upper passive wall, the condensate mass fraction occurs more upstream than that of the solid wall. This is due to the expansion waves generated from the slots of the porous wall.

In order to view the passive Prandtl-Meyer flow with condensation in more detail, a schematic diagram of the condensing flow field is made based upon the computational results, as shown in Fig. 8. The dotted line denotes the onset of condensation, and EW and CW refer to the expansion and compression waves, respectively, which are alternatively generated at the slots of the porous upper wall. At the most upstream slot on the upper wall, strong expansion

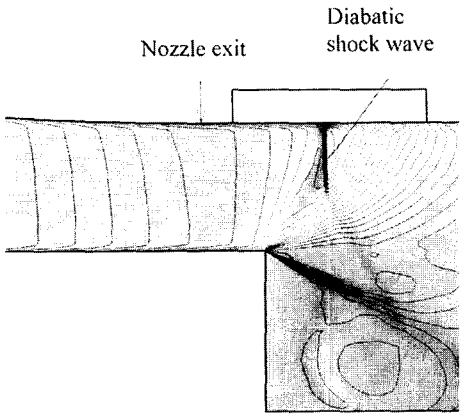

(a) Computed schlieren picture ($\Delta\rho/\rho_{01}=0.01$)

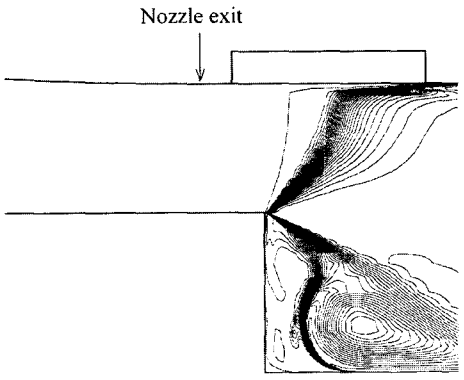

(b) Condensate mass fraction

Fig. 6 Computed schlieren picture and contour map of condensate mass fraction (Solid wall, $S_{01}=0.6$, $x_c=10$ mm)

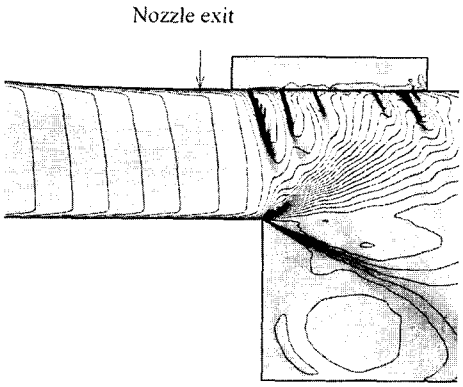

(a) Computed schlieren picture ($\Delta\rho/\rho_{01}=0.01$)

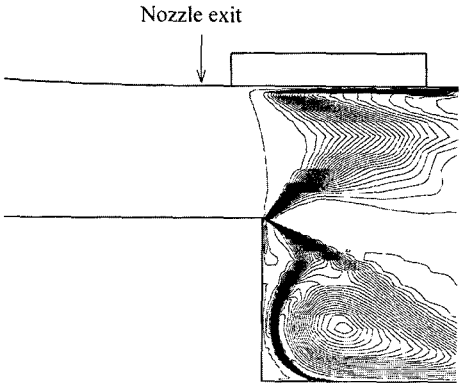

(b) Condensate mass fraction

Fig. 7 Computed schlieren picture and contour map of condensate mass fraction ($L=30$ mm, $S_{01}=0.6$, $x_p=5$ mm, $x_c=10$ mm)

waves is due to the flow breathing into the cavity, while at the most downstream slot, strong compression wave is due to the flow coming out from the cavity. The flow direction inside the cavity is left to right, as indicated in the arrows. It is found that for the passive upper wall, EW causes the onset of condensation near the upper wall to move upstream, compared with the solid wall. It is, thus, believed that the expansion waves play an important role in weakening the diabatic shock wave since the heat released by condensation are spatially distributed.

Figure 9 shows the unsteady behavior of the computed diabatic shock wave for solid wall, where T denotes the time of one cycle of oscillation. The computed density contour maps are taken during one cycle of self-excited oscillation. At $t=0.0T$, the diabatic shock wave due to condensation is located nearly at the nozzle exit and for time to increase, it moves upstream inside the convergent nozzle. At $t=0.4496T$, a new diabatic shock wave appears again inside the expansion fan downstream of the nozzle exit. As t increases, it moves upstream and at $t=0.8899T$, it is located just downstream of the nozzle exit. At $t=1.0T(=0.0T)$, one cycle of the diabatic shock motion is completed. In this case, the frequency of the unsteady periodic motion of diabatic shock wave is estimated to be $f=2.40$ kHz.

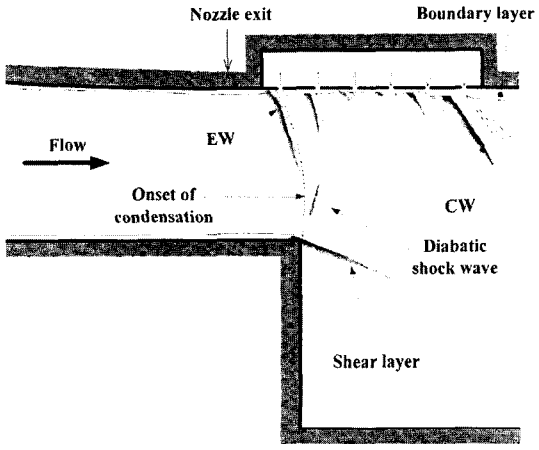

Fig. 8 Schematic diagram of passive Prandtl-Meyer flow ($L=30$ mm, $S_{01}=0.6$, $x_p=5$ mm, $x_c=10$ mm)

Note that the total temperature T_{01} and total pressure p_{01} in the upstream plenum are held constant at 298 K and 101.3 kPa, respectively, and $S_{01}=0.9$, $h^*=13$ mm, and $x_c=5$ mm. This unsteady periodic motion of diabatic shock wave was also found in supersonic nozzles (Wegener and Cagliostro, 1973; Matsuo et al., 1985).

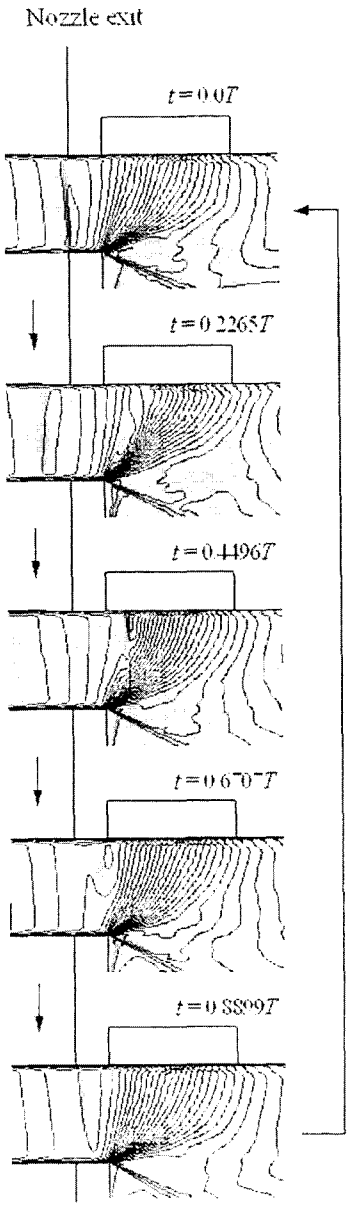

Fig. 9 Self-excited oscillation of diabatic shock wave ($h^*=13$ mm, Solid wall, $S_{01}=0.9$, $x_c=5$ mm, $f=2.40$ kHz)

For the same conditions as Fig. 9 above, Fig. 10 shows the computed time-histories of static pressure distributions along a horizontal line on the side-wall, which corresponds to the array of static holes in experiment. The arrow indicates the time to proceed. The static pressure distribution seems to be highly time-dependent. At a given time, the static pressure decreases with the distance, and it abruptly jumps when the flow meets the diabatic shock wave. Then it again decreases monotonously with the distance. With an increase in time, the static pressure jump moves upstream of the nozzle exit. A new pressure jump appears downstream of the nozzle exit, and it again moves upstream, thus completing a cyclic motion. This is due to the periodic excursion of the diabatic shock wave.

Figure 11 shows the computed time-histories of static pressure distributions for passive Prandtl-Meyer condensation flow, where $L=20$ mm, $x_c=5$ mm, and $x_p=5$ mm. It is interesting to note that the static pressure does not appreciably depend on time and no any appreciable oscillation in static pressure is found. It is clear that the passive upper wall suppresses completely the periodic oscillation of diabatic shock wave due to the heat addition process by condensation.

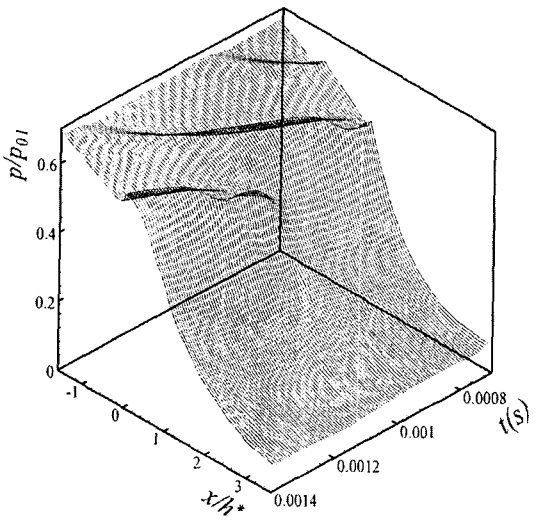

Fig. 10 Time histories of static pressure distributions ($h^*=13$ mm, Solid wall, $S_{01}=0.9$, $x_c=5$ mm)

Figure 12 presents a closer view of the passive Prandtl-Meyer expansion flow field described in Fig. 11. The density contour map shows that

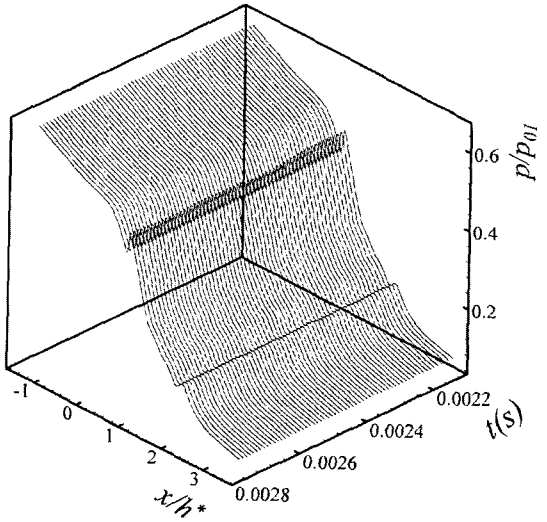

Fig. 11 Time histories of static pressure distributions ($h^*=13$ mm, $L=20$ mm, $S_{01}=0.9$, $x_p=5$ mm, $x_c=5$ mm)

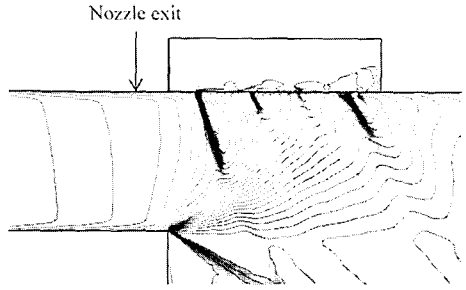

(a) Computed schlieren picture

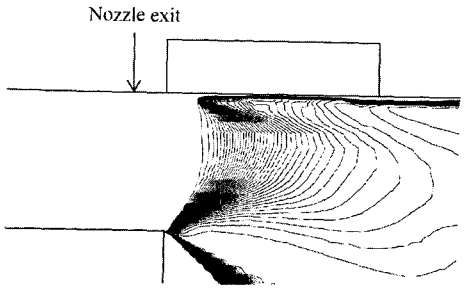

(b) Condensate mass fraction

Fig. 12 Computed schlieren picture and contour map of condensate mass fraction ($h^*=13$ mm, $L=20$ mm, $S_{01}=0.9$, $x_p=5$ mm, $x_c=5$ mm)

there is no appreciable diabatic shock wave and a multiple of the expansion and compression waves are generated from the slots of the porous upper wall. Over the cavity, the flow comes into the cavity through the slots upstream, while it comes out the cavity downstream, thereby leading to the cavity flow from the upstream toward the downstream field. The condensate mass fraction begins to increase rapidly close to the upstream slots on the upper porous wall and it is very large inside the expansion fan near the expansion corner and in the shear layers downstream of the backward-facing step. It is believed that the present porous wall and cavity system is very useful in alleviating the magnitude of the diabatic shock wave due to condensation as well as its unsteady periodic motions.

5. Conclusions

Prandtl-Meyer expansion flow with homogeneous condensation is investigated experimentally and by numerical computations. The steady and unsteady periodic behaviors of the diabatic shock wave due to the latent heat released by condensation are considered with a view of technical application to the condensing flow through steam turbine blade passages. A passive control method using a porous wall and cavity underneath is applied to control the diabatic shock wave, which occurs in Prandtl-Meyer expansion flow with condensation. The porous wall consists of a multiple of two-dimensional slots for the purpose of comparison with two-dimensional computational analysis, in which unsteady, compressible Navier-Stokes with the nucleation rate equation are numerically solved using a third-order TVD (Total Variation Diminishing) finite difference scheme. The computational results reproduce the measured static pressure distributions in passive and no passive Prandtl-Meyer expansion flows with condensation. From both the experimental and computational results, it is found that the magnitude of steady diabatic shock wave can be considerably reduced by the present passive control method. For no passive control, it is found that the diabatic shock wave oscillates periodically with a frequency of 2.40 kHz. This unsteady periodic motion of the diabatic shock wave can be completely suppressed using the present passive control method. The present experimented and computational results indicate that the passive control method using a porous wall and cavity system could be useful to control the condensing flow through steam turbine blade passages.

References

Adam, S. and Schnerr, G. H., 1997, "Instabilities and Bifurcation of Non-Equilibrium Two-Phase Flows," *Journal Fluid Mechanics*, Vol. 348, pp. 1~28.

Bahi, L., Ross, J. M. and Nagamatsu, H. T., 1983, "Passive Shock Wave/Boundary Layer Control for Transonic Airfoil Drag Reduction," AIAA Paper-83-0137.

Baldwin, B. S. and Lomax, H., 1978, "Thin Layer Approximation and Algebraic Model for Separated Turbulent Flows," AIAA paper 78-257.

Delale, C. F. and Crighton, D. G., 1998, "Prandtl-Meyer Flows with Homogeneous Condensation. Part 1, Subcritical Flows," *Journal of Fluid Mechanics*, Vol. 359, pp. 23~47.

Delale, C. F. and Crighton, D. G., 2001, "Prandtl-Meyer Flows with Homogeneous Condensation. Part 2, Supercritical Flows," *Journal of Fluid Mechanics*, Vol. 430, pp. 231~265.

Frank, W., 1979, "Prandtl-Meyer Expansion Mit Warmezufuhr," *Z. Angew. Math. Mech.*, Vol. 59, pp. 223~226.

Frank, W., 1985, "Condensation Phenomena in Supersonic Nozzles," *Acta Mechanica*, Vol. 54, pp. 135~156.

Kalra, S. P., 1975, "Experiments on Non-equilibrium, Nonstationary Expansion of Water Vapor/Carrier Gas Mixture in a Shock Tube," Univ. of Toronto, Institute of Aerospace Studies, Report 195.

Kawada, H. and Mori, Y., 1973, "A Shock Tube Study on Condensation Kinetics," *Bulletin of JSME*, Vol. 16, pp. 1053~1066.

Kurshakov, A. V., Saltanov, G. A. and

Tkalenko, R. A., 1971, "Theoretical and Experimental Investigation of Condensation in a Centered Rarefaction Wave," *Journal of Applied Mechanics and Technical Physics*, Vol. 12, No. 5, pp. 732~735.

Matsuo, K., Kawagoe, S., Sonoda, K. and Sakao, K., 1985, "Studies of Condensation Shock Waves (Part 1, Mechanism of Their Formation)," *Bulletin of JSME*, Vol. 28, pp. 2577~2582.

Matsuo, K., Kawagoe, S., Sonoda, K. and Setoguchi, T., 1985, "Oscillations of Laval Nozzle Flow with Condensation (Part 1)," *Bulletin of JSME*, Vol. 28, No. 241, pp. 1416~1422.

Peters, F., 1987, "Condensation of Supersaturated Water Vapor at Low Temperatures in a Shock Tube," *J. Phys*. Chem. Vol. 91, pp. 2487~2489.

Peters, F. and Paikert, B., 1989, "Nucleation and Growth Rates of Homogeneously Condensing Water Vapor in Argon from Shock Tube Experiments," *Experiments in Fluids*, Vol. 7, pp. 145~156.

Raghunathan, S. R., 1988, "Passive Control of Shock-Boundary Layer Interaction," *Prog. Aerospace Sci*., Vol. 25, pp. 271~296.

Schnerr, G. H., 1986, Homogene Kondensation in Sationaren Transsonischen Strömungen durch Lavaldusen und um Profile, Habilitationsschrift, Universitat Karlsruhe (TH), Germany.

Sislian, J. P. and Glass, I. I., 1976, "Conde nsation of Water Vapor in Rarefaction Waves, 1. Homogeneous Nucleation," *AIAA Jour*., Vol. 14, pp. 1731~1737.

Smith, L. T., 1971, "Experimental Investigation of the Expansion of Moist Air Around a Sharp Corner," *AIAA Jour*., Vol. 9, No. 10, pp. 2035~2037.

Walters, P. T., 1985, "Wetness and Efficiency Measurements in LP Turbines with an Optical Probe as an Aid to Improving Performance," Joint ASME/IEEE Conf. on Power Generation, Paper No. 85-JPGC-GT-9, Milwaukee.

Wegener, P. P. and Mack, L. M., 1958, "Condensation in Supersonic Hypersonic Wind Tunnels," Adv. in Applied Mechanics, Academic Press, Vol. 5, pp. 307~447.

Wegener, P. P. and Pouring, A. A., 1964, "Experiments on Condensation of Water Vapor by Homogeneous Nucleation in Nozzles," *Phys. of Fluids*, Vol. 7, pp. 352~361.

Wegener, P. P. and Cagliostro, D. J., 1973, "Periodic Nozzle Flow with Heat Addition," *Combustion Science and Technology*, Vol. 6, pp. 269~277.

White, A. J., Young, J. B. and Walters, P. T., 1996, "Experimental Validation of Condensing Flow Theory for a Stationary Cascade of Steam Turbine Blades," *Phil. Trans. Royal Society of London*, A, Vol. 354, pp. 59~88.

Yee, H. C., 1989, "A Class of High-Resolution Explicit and Implicit Shock-Capturing Methods," NASA TM-89464.